GEOPHYSICAL RESEARCH LETTERS, VOL. 35, L04606, doi:10.1029/2007GL032697, 2008

Self-regulation of deep-ocean internal wave continuum: Observations on related near-inertial shear and high-frequency vertical motions

Hans van Haren[1]

Received 16 November 2007; revised 9 January 2008; accepted 15 January 2008; published 21 February 2008.

[1] It is shown using detailed yearlong acoustic current observations between 850 and 1350 m that large-scale and small-scale waves in the ocean interior are coupled in a self-regulating fashion. Vertical current shear, a key to vertical mixing, is dominated near the local inertial frequency. Its value follows details of maximum buoyancy frequency 'N_{max}' in thin layers of different density. Its frequency however, is determined by the minimum N_{min} in the near-homogeneous layers between the N_{max}-layers. These weakly stratified layers are maintained by overturning of density surfaces due to high-frequency internal waves guided by the shear-layers. Rare vertical current observations show a spectral continuum between [N_{min}, N_{max}] of low-mode interfacial waves rather than wave-groups propagating through smooth large-scale stratification. **Citation:** van Haren, H. (2008), Self-regulation of deep-ocean internal wave continuum: Observations on related near-inertial shear and high-frequency vertical motions, *Geophys. Res. Lett.*, *35*, L04606, doi:10.1029/2007GL032697.

1. Introduction

[2] The ocean interior is generally stable density stratified in the vertical, which hampers vertical exchange of heat, momentum and suspended matter. However, the same density stratification can support 'internal gravity wave' (IW) propagation [*Ekman*, 1931] in three dimensions. These waves are thought to dominate limited vertical diapycnal exchange [*Gregg*, 1987], presumably via the breaking of small-scale internal waves upon shear or convective instabilities induced by large-scale waves. The precise mechanism of coupling between large- and small-scale internal waves and the dynamics behind the internal wave spectrum are still unknown. In this paper, some particulars of the relation between internal waves at different frequencies are demonstrated using yearlong time-series of acoustic Doppler current profiler (ADCP) observations. The data range across 500 m around ~3200 m above the bottom in the vicinity of Great Meteor Seamount, an underwater volcano in the North-Atlantic Ocean.

[3] At such distance from the bottom, topography is not expected to significantly modify the IW-band from its typical open ocean structure as its influence by enhancing particular IW-energy due to critical reflection is observed to range less than 700 m above the bottom [*Eriksen*, 1998]. Nonetheless, topography does modify the internal wave band as it promotes generation of internal tides, one of the dominant IW-sources. A second mechanical source has large response of generally horizontal motions near the local inertial frequency $f = 2\Omega\sin\varphi$, the vertical component of the Earth rotational vector Ω at latitude φ. Inertial motions result from geostrophic adjustment, e.g., following the passage of atmospheric disturbances or relaxation of internal fronts. Traditionally, the IW-band is defined between frequencies (σ) $f < \sigma < N$, where N denotes the buoyancy frequency at which nearly vertical motions are found. Outside this frequency range, waves are basically evanescent motions, exponentially decaying in amplitude, except when N = O(f) and the more general inertio-gravity wave 'IGW' band extends beyond the above limits to [$\sigma_{lo}(N) < f$, $\sigma_{hi}(N) > N$] due to the effects of the horizontal component $f_h = 2\Omega\cos\varphi$ [*LeBlond and Mysak*, 1978].

[4] In a well- and smoothly stratified ocean, the motions at the two extremities of the IW-band show similar behavior of interior enhancement near 'turning points', which can be described using Airy functions [*Desaubies*, 1973]. Using these functions and vertical somewhat arbitrarily chosen mode-4 wave packets small enough to propagate within a wave-guide set by the large buoyancy scale, so that maximum wave frequency is $1/2N_{max}$, *Munk* [1980] demonstrated this similar behavior near turning latitudes and depths for f- and N-motions, respectively. However, he did not couple f- and N-motions, which, perhaps, is not possible in a smoothly varying stratified ocean.

[5] Therefore, the viewpoint in this paper will be a step-like, non-smoothly varying stratified ocean, as observed by, e.g., *Cooper and Stommel* [1968]. The vertically rapidly varying stratification is set-up by straining due to internal waves but otherwise assumed in equilibrium, following theoretical suggestions [*Orlanski and Bryan*, 1969] and near-surface temperature observations [*Brekhovskikh et al.*, 1975]. Also, vertical mode-1 is allowed so that coherent vertical motions across vertical scales much larger than the large buoyancy scale and motions at density step $N = N_{max}$ can exist, in principle. So far, low-mode near-N motions have mainly been observed using near-surface temperature observations over short periods of time, e.g., in shelf seas [*Halpern*, 1971], near the equator [*Moum et al.*, 1992] and in lakes [*Antenucci and Imberger*, 2001]. These near-surface high-frequency internal waves are likely induced by wind, e.g. via wave-wave interaction [*Phillips*, 1966], but the precise generation was not established.

[6] Here, internal waves are observed using a four-beam ADCP, which is the only type of moored oceanographic equipment that can monitor the entire IGW-band from purely horizontal motions near the lower frequency bound to vertical motions near the upper bound. As it measures the three current components (u,v,w), or (east, north, vertical), and a non-Cartesian error velocity 'e' at different depth

[1]Royal Netherlands Institute for Sea Research, Den Burg, The Netherlands.

0094-8276/08/2007GL032697$05.00

Table 1. RDI-Broadband Uplooking-ADCP Mooring Details Above the Foot of Great Meteor Seamount in the North-Atlantic Ocean

Details	Description
Data start	19/10/2004
Data end	15/12/2005
Latitude	30°00′N
Longitude	−027°48′W
Water depth (m)	4550
Vertical slant angle (θ)	20°
Transmit frequency	75 kHz
Transmission length	28 m
Instrument depth	3180 m above bottom
First bin	1332 m
# bins × vertical bin size	50 × 10 m
Ensemble period	900 s
Std u, v	0.014 m s^{-1}/ens
Std w, e	0.005 m s^{-1}/ens

levels, it can also resolve vertical shear of horizontal currents, which is important for mixing, and it gives a direct noise-estimate to w, via e. We compute vertical current shear $\mathbf{S} = (\Delta u/\Delta z, \Delta v/\Delta z)$ across vertical scales Δz rather than kinetic energy to be representative of IW(f) and we use rare w-observations rather than potential energy to measure IW(N).

2. Data

[7] Table 1 lists instrumental details of the 14 months mooring deployment including an ADCP that was mounted in the top-buoy of a 3000 m long mooring. Pressure and tilt sensor information show that mooring motions caused top-buoy position deviations of less than 1.2 m in the vertical and less than 100 m in horizontal directions. This little mooring motion is due to the use of a thin, 0.007 m in diameter, steel mooring cable and two large, elliptically shaped, low-drag elements providing ∼400 kg total net buoyancy. The maximum deviation in the horizontal is comparable with the bounds of horizontal beam spread, which varies between 15 and 300 m over the ADCP's range. This spread is comparable to typical near-surface short-wavelength estimates of 150–250 m by *Halpern* [1971] and *Moum et al.* [1992], but well less than a mean of 1350 m estimated for "long-wave" near-surface solitary waves by *New and Da Silva* [2002]. Due to a relative lack of scatterers, the lower 150 m of the ADCP-range showed noisier w-data, by up to a factor of 3 larger than higher-up, so that w(N) did not stand out of the noise at these larger depths (Figure 1).

3. Observations

[8] At ∼1000 m, open ocean vertical current shear is clearly organized in thin layers, about 25 m in thickness and more or less horizontal, little varying with depth (Figure 1a). This resembles near-surface observations. The relatively small vertical excursion (amplitude ∼ one layer thickness) of these layers has a semidiurnal tidal periodicity that also dominates the kinetic energy. However, this tidal energy varies on rather large vertical scales O(1000 m), as inferred using current meters below the ADCP. In contrast, the shear is predominantly found at f, due to the small vertical scales of the layering [*van Haren*, 2007a]. Instead of horizontal layers, the vertical current is organized in high-frequency vertical bands, or low vertical mode, that basically range across at least 500 m to first order (Figure 1b). To second order, sub-maxima in w occur in layers similarly to the shear-layering, albeit not always at precisely the same depth. This suggests support of these waves by thin layers. As a result, the present data, although being depth-time series, confirm the general conception that the internal wave band ranges from horizontally organized near-inertial motions to vertically organized near-buoyancy motions.

[9] Stratification decreases towards the bottom, by almost a factor of two across the ADCP-range, although many small-scale step-layers in density are observed throughout the water column (Figure 2a). These steps have roughly the same scale of layering as the near-inertial shear. Smoothed large-scale (Δz = 100 m) buoyancy period values vary between $T_N \approx 1500-4000$ s across the range of the ADCP (Figure 2b). $T_N > 2$ h values are found in thin 'homogeneous' layers and $T_N < 1000$ s in even thinner stratified layers (small-scale Δz = 1 m). The coupling between the low- and high-frequency motions in the internal wave band

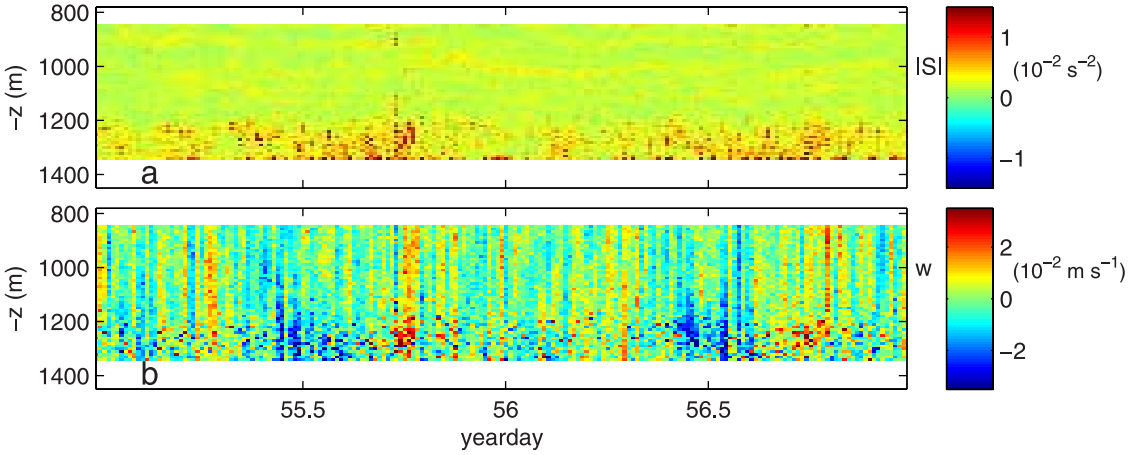

Figure 1. Two arbitrary days of detail time-depth series from raw ADCP-data. Poorer, erratic data are found below ∼1200 m. (a) Vertical current shear magnitude computed using Δz = 10 m. The colour coding includes negative values for display purposes. (b) Vertical current ADCP-data.

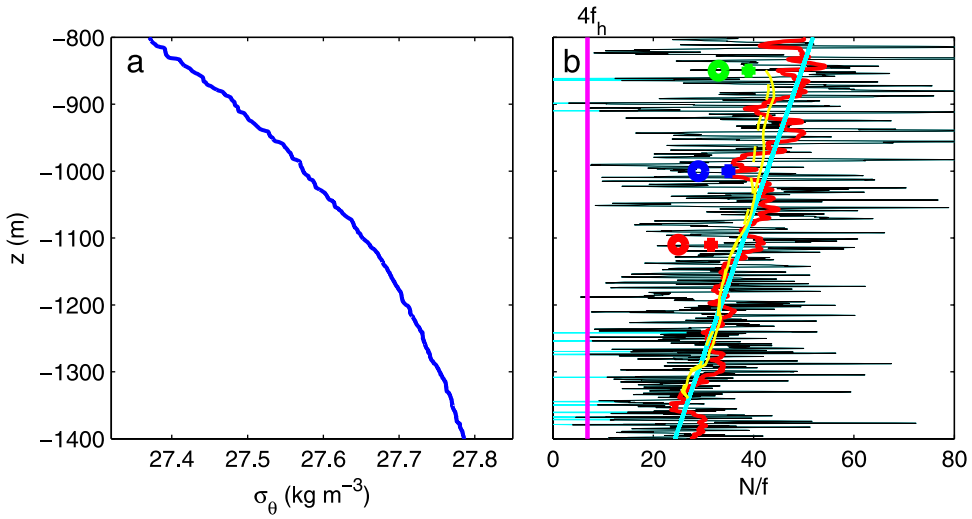

Figure 2. (a) Sigma-theta (relative density) versus depth from CTD obtained just before mooring deployment. (b) Buoyancy frequency computed from CTD-data using $\Delta z = 1$ m (black), excluding convectively unstable values (in light-blue unstable values, mainly below 1200 m), and $\Delta z = 100$ m (red). The sloping blue line is the linear best-fit to the data in the window. The open circle indicates the near-N peak frequency in the w-spectra (Figure 3b) at three arbitrary depths whilst the cross indicates the associated kinetic energy peak frequency (Figure 3c). The yellow curves denote half the overall mean current variance for u(solid) and v(dashed), with scale in 10^{-4} m^2 s^{-2}.

is seen using the vertical (and temporal) variations in density stratification for guidance.

[10] In yearlong average spectra, vertical and horizontal current variance in the internal wave band is dominated by non-linear higher harmonics of tidal motions and inertial-tidal interactions, and countable as separate deterministic peaks up to 8–10 times per day (Figure 3). For the vertical currents only, substantial part of the diurnal and its higher harmonic motions is due to zooplankton migration, which occurs also at these great depths well below the photic zone [*Plueddemann and Pinkel*, 1989; *van Haren*, 2007b]. The near-inertial "peak" is smoothed across a moderately broad band consisting of non-significant sub-peaks, with a tendency to be shifted to sub-inertial frequencies for shear (Figure 3a). The near-inertial shear peak becomes narrower with increasing depth, and, just like the *total* current variance (Figure 2b), the square root of the yearlong mean shear-variance averaged over the near-inertial band matches very closely the large-scale N(z) variation, in ratio 1:0.85:0.76 ± 0.0015 for depths 850, 1000, 1110 m, respectively. Even broader seems a band 'peaking' near large-scale N, which is observed most clearly in w (Figure 3b) but also in horizontal kinetic energy (Figure 3c). Finally, the broadest band is the rest of the internal wave band continuum, which is more or less flat in w, but sloping at a canonical rate of −1 in frequency for horizontal currents. Thus, the aspect ratio of continuum (not tidal harmonics) $|w|/(|u|^2 + |v|^2)^{1/2} = 0.5 \pm 0.1$ near N and 10 ± 3 around f.

[11] Besides through the equivalence of large-scale shear and buoyancy frequency, the internal wave coupling follows from a series of new observations in the spectra. With the vertical variation in N it is seen that the spectra shrink in frequency, equally for vertical and horizontal motions. However, vertical near-N motions peak at N-6 cpd, which is about 1 std(N) (standard deviation of mean N) lower than mean *large*-scale N (Figure 2b) whilst horizontal motions peak at slightly higher frequencies N-0.5 std (N-3 cpd). The average near-N peak frequencies in w $\sigma_p(\sim N) \approx 1/2N_{max}(\Delta z \approx 10$ m). These peak frequencies conform to the potential energy model of *Munk* [1980] and match the aspect ratio of currents observed here. The broadness of the near-N band extends, however, towards the same *small*-scale N_{max}, although being barely resolved in the present data. With w-motions up to N_{max}, one expects also motions down to small-scale $N_{min} \approx 5–10f$ (Figure 2b). Indeed, disregarding the deterministic peaks, the continuum w-spectra extend significantly above noise level for $\sigma > 6.5 \pm 1f$, which is close to $4f_h = 6.9f$ at this latitude (Figure 3b). It is noted that this N_{min}-range is independent of z, in contrast to N(z) and $N_{max}(z)$, as the depth-order is irregular compared to that of peak-frequencies near the N-bulge. Within $[4f_h, N_{max}]$ w-motions are predominantly low-vertical mode across the ADCP-range also when the aspect ratio becomes smaller, as has been verified using different band-pass filters.

[12] This frequency range also bounds the statistical distribution of small-scale (1-m) N, which for the range [800, 1400] m has the same shape as the w-continuum spectrum including a sub-peak near 10f (Figure 3b). The similarity between spectral and statistical distributions suggests a long-term similar distribution "balance" between high-frequency internal waves and strained stratification, but the $N_{min} = 4f_h$ suggest another coupling.

[13] At such low buoyancy frequencies the internal wave band measurably differs from traditional bounds [f, N] to IGW-bounds $[\sigma_{lo}(4f_h), \sigma_{hi}(4f_h)] \approx [0.97f, 1.03N]$ due to the effects of the horizontal Coriolis force component in the weakly stratified layers [*LeBlond and Mysak*, 1978]. The lower-frequency extension of this IGW is best seen in

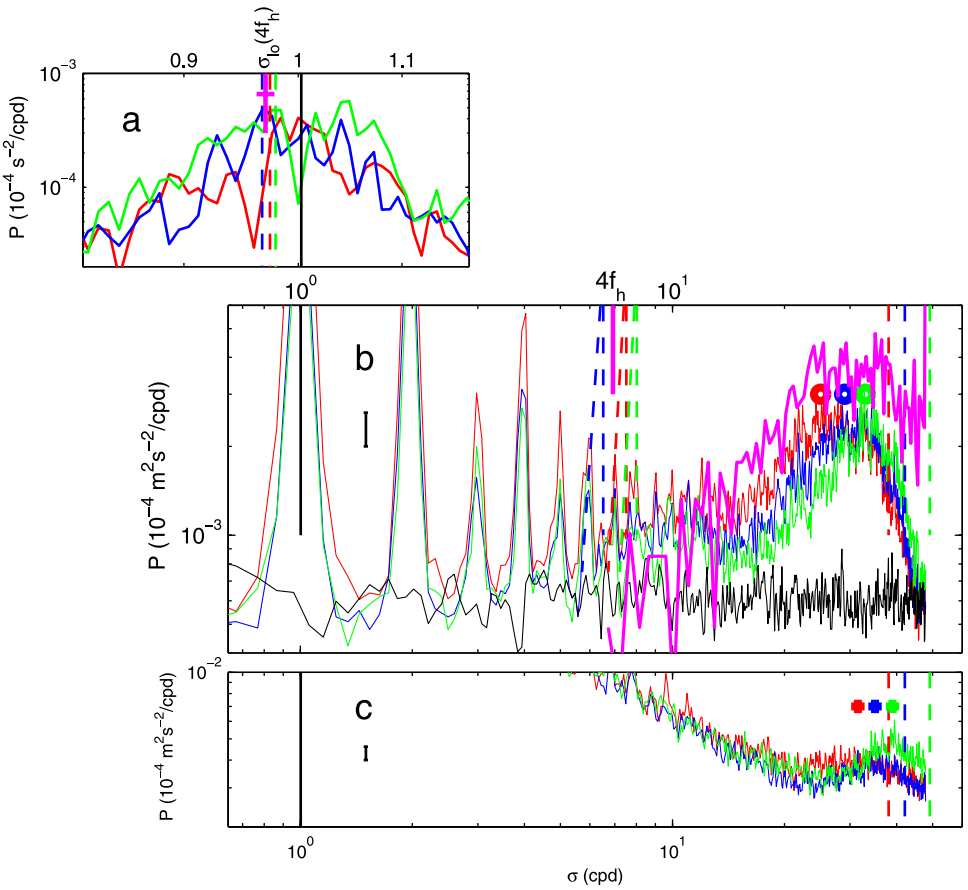

Figure 3. Spectra from 14 months of ADCP-data at three depths indicated in their colours in Figure 2b. (a) Near-f detail of nearly raw shear. The vertical lines indicate IGW-$\sigma_{lo}(N_{min})$ using N_{min} from Figure 3b; the purple bar around $4f_h$ indicates the equivalent fundamental bandwidth. (b) Smoothed internal wave band w. For reference in black the spectrum of white noise is given, measured at 1110 m. The set of vertical dashed lines near $4f_h$ indicates local N_{min} where w reaches white noise 'e.' These N_{min} are used to compute the sub-inertial lower IGW-bounds in Figure 3a; the set of vertical lines to the right indicates the local mean N that are computed from CTD-data in Figure 2b using the linear best-fit. In purple, the statistical histogram distribution is shown of small-scale N(Δz = 1 m) over the depth-range of Figure 2b. (c) Smoothed kinetic energy focusing on near-N part.

shear, which peaks at those sub-inertial frequencies that are associated with w(N_{min}) via $\sigma_{lo}(N_{min})$, see Figure 3. Thus, whilst shear *values* follow the details of small-scale N by keeping maximal stress on N_{max}-layers, thereby creating the wave-guide for maximum growth of near-interface-scale-N $\approx$ interface-scale-$|\mathbf{S}|$ motions as observed in the North Sea [*van Haren*, 2005], the shear *frequency* follows N_{min} = $4f_h$, presumably due to the trapping of sub-inertial motions or, perhaps, due to mixing and straining generated following the passage of a train of high-frequency (solitary) waves [*Helfrich and Melville*, 2006].

4. Discussion

[14] The self-regulation mechanism between destabilizing shear, high-frequency wave motion and stabilizing stratification suggests a subtle balance between the originally smoothly varying buoyancy input and the regular (tides) and irregular (inertial motions) kinetic energy input. The responses to the latter appear intermittently following geostrophic adjustment of irregularly passing disturbances. An initially smooth buoyancy profile can support internal waves, which, by virtue of their grouped propagation, create variable enhanced and decreased 'step-like' stratification by straining. Then, the balance between high vertical mode, low-frequency shear and low vertical mode, high-frequency internal waves determines (1) the internal wave band extent including frequency limits for vertical current continuum and sub-inertial shear (small-scale N, Δz = O(1 m), which is one decade smaller than the canonical roll-off scale for ocean shear [*Gargett et al.*, 1981]), (2) kinetic energy and shear levels (small-scale N_{max} that determines large-scale N $\approx$ large-scale $|\mathbf{S}|$, Δz = O(100 m)), (3) the waveguide for the irregularly occurring low-mode N-motions (medium-scale |S|, Δz = 2A = O(10 m), A denoting the amplitude of high-frequency waves [*van Haren*, 2005]), (4) a spectral extent for w (and potential and kinetic energy) continuum which precisely matches the N-statistics distribution across the relevant vertical range of the large-scale N (Figure 3b) for short-scale [N_{min}, N_{max}], thereby confirming the built-up of the spectrum by low-mode interfacial waves and the long-term equilibrium between density steps and high-frequency internal waves.

[15] The linear near-N waves within their waveguide will move in equilibrium with their [shear]guide up to breaking [*Phillips*, 1966]. Due to their low-mode character, such wave motions also occur in layers where small-scale N < waveguide-scale $|\mathbf{S}|$. As a result, these motions will initiate overturning, thereby maintaining the weak local N_{min}. In the North Sea, variation with time occurs for maximal near-N waves upon near-f shear *collapse*, so that the two set-up a new equilibrium with lower large-scale N [*van Haren*, 2005]. Likewise in a similar sea, the near-N temperature spectral extent attributed to solitary waves varies its peak frequency with N(z) [*Halpern*, 1971].

[16] Here, in the ocean well below any direct influence of atmospheric disturbances, the large-scale N variation with depth seems permanent, but the environment changes continuously with time. Even slowly varying near-inertial shear does vary on a time scale of a few days. The thin stratified layers are moved up and down by other internal waves like internal tides. As a result, the dynamic environment occasionally allows for generation of packets of low-mode waves close to the buoyancy frequency and which are suggested to develop as highly non-linear internal solitary waves [e.g., *Halpern*, 1971; *Helfrich*, 1992] eventually dissipating upon shoaling or reaching their stability limit [*Lamb*, 2002; *Xing and Davies*, 2007], thereby causing diapycnal mixing. In the present open ocean data this happens seldom and is not well observed, presumably because topography is far away. A natural limiting frequency seems $N_{min} = 4f_h$, for which shear creates a convective environment that becomes distorted by the Earth's rotational vector, being no longer precisely vertical. Noting that near-inertial motions are the only motions that can penetrate vertically through a step-like density stratified oceans, no matter how small their spatial scales, it is not surprising that these motions are observed to dominate ocean shear.

[17] In addition, the present series of internal wave continuum motions show low vertical mode-1 or -2 vertical currents spanning a substantial part, several 100 m, the 'large-scale', of the water column. Although the 'waves' have relatively small horizontal extent, they are coherently measured using relatively large O(10–100) m horizontally spread ADCP-instrumentation.

[18] **Acknowledgments.** The assistance of the crew of R/V Pelagia is highly appreciated. Theo Hillebrand provided indispensable assistance in mooring preparation. Long-term Ocean Climate Observations (LOCO, some of which are the GMS-observations) is funded in part by the Netherlands Organization for the advancement of Scientific Research (NWO).

References

Antenucci, J. P., and J. Imberger (2001), On internal waves near the high-frequency limit in an enclosed basin, *J. Geophys. Res.*, *106*, 22,465–22,474.

Brekhovskikh, L. M., K. V. Konjaev, K. D. Sabinin, and A. N. Serikov (1975), Short-period internal waves in the sea, *J. Geophys. Res.*, *80*, 856–864.

Cooper, J. W., and H. Stommel (1968), Regularly spaces steps in the main thermocline near Bermuda, *J. Geophys. Res.*, *71*, 5849–5854.

Desaubies, Y. J. F. (1973), Internal waves near the turning point, *Geophys. Fluid Dyn.*, *5*, 143–154.

Ekman, V. W. (1931), On internal waves, *Rapp. P. V. Réun. Cons. Int. Explor. Mer*, *76*, 5–31.

Eriksen, C. C. (1998), Internal wave reflection and mixing at Fieberling Guyot, *J. Geophys. Res.*, *103*, 2977–2994.

Gargett, A. E., P. J. Hendricks, T. B. Sanford, T. R. Osborn, and A. J. Williams (1981), A composite spectrum of vertical shear in the upper ocean, *J. Phys. Oceanogr.*, *11*, 1258–1271.

Gregg, M. C. (1987), Diapycnal mixing in the thermocline: A review, *J. Geophys. Res.*, *92*, 5249–5286.

Halpern, D. (1971), Observations on short-period internal waves in Massachusetts Bay, *J. Mar. Res.*, *29*, 116–132.

Helfrich, K. R. (1992), Internal solitary wave breaking and run-up on a uniform slope, *J. Fluid Mech.*, *243*, 133–154.

Helfrich, K. R., and W. K. Melville (2006), Long nonlinear internal waves, *Annu. Rev. Fluid Mech.*, *38*, 395–425.

Lamb, K. G. (2002), A numerical investigation of solitary internal waves with trapped cores formed via shoaling, *J. Fluid Mech.*, *451*, 109–144.

LeBlond, P. H., and L. A. Mysak (1978), *Waves in the Ocean*, 602 pp., Elsevier, New York.

Moum, J. N., D. Hebert, C. A. Paulson, and D. R. Caldwell (1992), Turbulence and internal waves at the equator. Part I: Statistics from towed thermistors and a microstructure profiler, *J. Phys. Oceanogr.*, *22*, 1330–1345.

Munk, W. H. (1980), Internal wave spectra at the buoyant and inertial frequencies, *J. Phys. Oceanogr.*, *10*, 1718–1728.

New, A. L., and J. C. B. Da Silva (2002), Remote-sensing evidence for the local generation of internal soliton packets in the central Bay of Biscay, *Deep Sea Res., Part I*, *49*, 915–934.

Orlanski, I., and K. Bryan (1969), Formation of the thermocline step structure by large-amplitude internal gravity waves, *J. Geophys. Res.*, *74*, 6975–6983.

Phillips, O. M. (1966), *The Dynamics of the Upper Ocean*, 261 pp., Cambridge Univ. Press, Cambridge, U. K.

Plueddemann, A. J., and R. Pinkel (1989), Characterization of the patterns of diel migration using a Doppler sonar, *Deep Sea Res., Part A*, *36*, 509–530.

van Haren, H. (2005), Internal waves near the buoyancy frequency in a narrow wave-guide, *J. Sea Res.*, *53*, 121–129.

van Haren, H. (2007a), Shear at the critical diurnal latitude, *Geophys. Res. Lett.*, *34*, L06601, doi:10.1029/2006GL028716.

van Haren, H. (2007b), Monthly periodicity in acoustic reflections and vertical motions in the deep ocean, *Geophys. Res. Lett.*, *34*, L12603, doi:10.1029/2007GL029947.

Xing, J., and A. M. Davies (2007), On the importance of non-hydrostatic processes in determining tidally induced mixing in sill regions, *Cont. Shelf Res.*, *27*, 2162–2185.

H. van Haren, Royal Netherlands Institute for Sea Research, P.O. Box 59, NL-1790 AB Den Burg, The Netherlands. (hansvh@nioz.nl)